AGU PUBLICATIONS

JGR

Journal of Geophysical Research: Space Physics

RESEARCH ARTICLE
10.1002/2015JA021144

Special Section:
Long-term Changes and Trends in the Stratosphere, Mesosphere, Thermosphere, and Ionosphere, JGR-Atmospheres/Space Physics, 2014

Key Points:
- PMSE periodicities of 7 and 9 days characterize solar minimum years
- CIR/HSS-driven geomagnetic disturbances induce strong *D* region ionization
- PMSE is sensitive to the impact of CIR/HSS-driven geomagnetic disturbances

Correspondence to:
Y.-S. Lee,
youngsooklee@kasi.re.kr

Citation:
Lee, Y.-S., S. Kirkwood, Y.-S. Kwak, G. G. Shepherd, K.-C. Kim, T.-Y. Yang, and A. Kero (2015), Characteristics of PMSE associated with the geomagnetic disturbance driven by corotating interaction region and high-speed solar wind streams in the declining solar cycle 23, *J. Geophys. Res. Space Physics*, *120*, 3198–3206, doi:10.1002/2015JA021144.

Received 19 FEB 2015
Accepted 21 MAR 2015
Accepted article online 25 MAR 2015
Published online 22 APR 2015

Characteristics of PMSE associated with the geomagnetic disturbance driven by corotating interaction region and high-speed solar wind streams in the declining solar cycle 23

Young-Sook Lee[1], Sheila Kirkwood[2], Young-Sil Kwak[1,3], Gordon G. Shepherd[4], Kyung-Chan Kim[1], Tae-Yong Yang[1,3], and Antti Kero[5]

[1]Korea Astronomy and Space Science Institute, Daejeon, South Korea, [2]Swedish Institute of Space Physics, Kiruna, Sweden, [3]Department of Astronomy and Space Science, University of Science and Technology, Daejeon, South Korea, [4]Centre for Research in Earth and Space Science, York University, Toronto, Ontario, Canada, [5]SGO, University of Oulu, Tähteläntie, Finland

Abstract We report interannual variations of the correlation between the reflectivity of polar mesospheric summer echoes (PMSEs) and solar wind parameters (speed and dynamic pressure), and *AE* index as a proxy of geomagnetic disturbances, and cosmic noise absorption (CNA) in the declining phase (2001–2008) of solar cycle 23. PMSEs are observed by 52 MHz VHF radar measurements at Esrange (67.8°N, 20.4°E), Sweden. In approaching the solar minimum years, high-speed solar wind streams emanate from frequently emerging coronal holes, leading to 7, 9, and 13.5 day periodicities in their arrival at Earth. Periodicities of 7 and/or 9 days are found in PMSE reflectivity in 2005–2006 and 2008. Periodicity-resolved correlations at 7 and 9 days of both *D* region ionization observed by cosmic noise absorption (CNA) and PMSE with solar wind speed and *AE* index vary from year to year but generally increase as solar minimum is approached. PMSEs have a higher periodicity-resolved correlation with *AE* index than the solar wind speed. In addition, cross correlation of PMSE reflectivity with *AE* index is mostly higher than with CNA in solar minimum years (2005–2008). This can signify that high-speed solar wind stream-induced high-energy particles possibly have strong influence on CNA, but not as much as on PMSE, especially for the years of significant periodicities occurring.

1. Introduction

The occurrence and intensity of polar mesospheric summer echoes (PMSEs), usually observed at altitudes of 80–90 km, are expected to be sensitive to several atmospheric and ionospheric parameters, including electron density, its gradient, charged ice particle number density, turbulent energy dissipation rate, viscosity, and temperature [*Ecklund and Balsley*, 1981; *Cho and Röttger*, 1997; *Varney et al.*, 2011, and references therein]. Based on the importance of ionospheric parameters in producing PMSE, the relationship of PMSE with geomagnetic disturbances has been examined in the literature. Using magnetic disturbance indices such as *K*, *Kp*, *Ap*, and *AE*, a clear influence on PMSE has been found, although varying from year to year [*Bremer et al.*, 2000; *Barabash et al.*, 2002; *Zeller and Bremer*, 2009; *Kirkwood et al.*, 2013; *Smirnova et al.*, 2011]. Recently, it has been found that high-speed solar wind stream (HSS)-induced geomagnetic disturbances are likely followed by an increased production of PMSE [*Lee et al.*, 2013, 2014]. The HSS-differentiated effect on PMSE is attributed to a large increase in high-energy electrons and relativistic electrons penetrating into the polar middle atmosphere during HSS [e.g., *Baker et al.*, 1987; *Rostoker et al.*, 1998; *Meredith et al.*, 2011; *Newnham et al.*, 2011; *Kavanagh et al.*, 2012]. HSS emanate up to 700–800 km s^{-1} from solar coronal holes and increase in number in approaching the solar minimum years [*Krieger et al.*, 1973; *McComas et al.*, 2002]. As the fast stream catches up with and overtakes the slow stream (~350 km s^{-1}) of the ambient solar wind, interaction regions are formed at 1 AU near the Earth's magnetopause in spiral shapes wrapping around the Sun, so-called corotating interaction regions (CIRs) [*Smith and Wolfe*, 1976; *Pizzo*, 1985]. Since the interplanetary magnetic fields are highly variable within CIRs due to compression by the HSS, CIRs usually create geomagnetic storms with $Dst < -100$ nT [*Tsurutani et al.*, 1995; *Tsurutani and Gonzalez*, 1997; *Echer et al.*, 2008]. Owing to coronal holes usually being long lasting, HSS/CIR-driven storms last for several days, in contrast to more transient coronal mass ejection-driven storms [*Blake et al.*, 1992]. The increase of relativistic electrons (>0.5 MeV), which reaches a

maximum in solar minimum years in geosynchronous orbit, is attributed to Pc5 ULF wave increases during HSS [e.g., *Li et al*., 1997; *Rostoker et al*., 1998; *Elkington et al*., 1999; *Kim et al*., 2006].

By examining the periodic correlation between HSS and PMSE occurrence/intensity, it is possible to test the reliability of the proposal that *D* region ionization caused by the HSS-induced precipitating high-energy particles facilitates PMSE formation [e.g., *Longden et al*., 2008; *Lee et al*., 2013]. Whether PMSE is directly linked to *D* region ionization is still obscure since inconsistent results have been reported regarding the correlation between cosmic noise absorption (CNA) as a proxy of *D*/*E* region ionization and PMSE, sometimes positive [e.g., *Morris et al*., 2005], sometimes negative [*Barabash et al*., 2002].

Periodic variations in the thermosphere associated with HSS have previously been reported by *Lei et al*. [2008a, 2008b]. In this study, first, the interannual variation of the same periodicities (7 and 9 days) of PMSE and CNA is observed in the declining phase of solar cycle 23, from 2001 to 2008. We examine whether the HSS effect, as on the *F* region ionosphere, increases in approaching the solar minimum years for both *D* region ionization and PMSE. Second, it is interesting to see how correlations of PMSE with solar wind parameters (speed and dynamic pressure) and *AE* index as a proxy of geomagnetic disturbance level, with *D* region ionization and with temperature, vary in the solar declining cycle. This study proceeds as follows. In section 2, data observations for PMSE and CNA are described. In section 3.1, PMSE periodicities are compared with those of solar wind speed, solar wind dynamic pressure, *AE* index, and CNA. In section 3.2, cross correlations between PMSE and the solar wind parameters, and between PMSE and CNA, are examined. In section 4, the discussion and conclusions are described.

2. Data Analysis

The Esrange mesosphere-stratosphere-troposphere radar (ESRAD) is an atmospheric radar located at Esrange, Sweden (67.8°N, 20.4°E; magnetic latitude 64.75°N), providing information on the dynamic state of the atmosphere—winds, waves, turbulence, and layering. The ESRAD data, available since July 1996, are measured at a frequency of 52 MHz corresponding to a wavelength of 5.77 m, well suited to monitor the atmospheric structures at about 3 m scale up to the mesosphere. The radar has six spaced receivers in two rows aligned to the east-west direction to record backscattered signals. A technical description of ESRAD is provided in *Chilson et al*. [1999]. Volume reflectivity (η), the radar cross section per unit volume of the atmosphere, is an intrinsic property of the atmospheric scatterers and can be calculated from the echo power detected by the radar after correcting for all instrumental effects. More information can be found in *Kirkwood et al*. [2013]. As a measure of PMSE intensity, volume reflectivity (η) is derived here from the so-called "fca_4500" mode with 600 m height resolution. The fca_4500 mode is easy to calibrate accurately, and the hourly averaged data have been used in earlier studies of the year-to-year variation of PMSE.

CNA is a proxy of *D*/*E* region ionization induced by precipitating particles. It represents the height-integrated absorption of cosmic noise by electron density increased above a quiet background level between heights of about 60 and 120 km, with the relative contribution from different heights depending on the height profile of the ionization and background neutral atmosphere temperature and pressure. CNA used here is measured using the La Jolla fast-response solid-state riometer operated at 30 MHz [*Hunsucker*, 1991], which is located in Abisko (68°.24′N, 18°.54′E). The cosmic noise absorption (*A*) in decibel (dB) has been calculated to derive hourly and daily averages for each summer according to

$$A = 10 \log_{10}(P_0/P),$$

where P_0 is the power output for a quiet day and P is the signal power output of the riometer. The quiet day curves are estimated for each day individually based on the median values of the previous 10 days. P_0 depends on the direction of the antenna relative to the stars, and it changes in a cyclic manner due to the rotation of the Earth (with a period corresponding to the sidereal day). The solar wind parameter is obtained for hourly and daily averages from OMNIWeb (http://omniweb.gsfc.nasa.gov/form/omni_min.html). Daily-averaged temperature data are obtained for 87 km height, 64°N–72°N latitudes and 0°E–40°E longitudes from Microwave Limb Sounder (MLS) measurements on the Aura spacecraft, available at http://mirador.gsfc.nasa.gov/cgi-bin/mirador/presentNavigation.pl?tree=project&project=MLS.

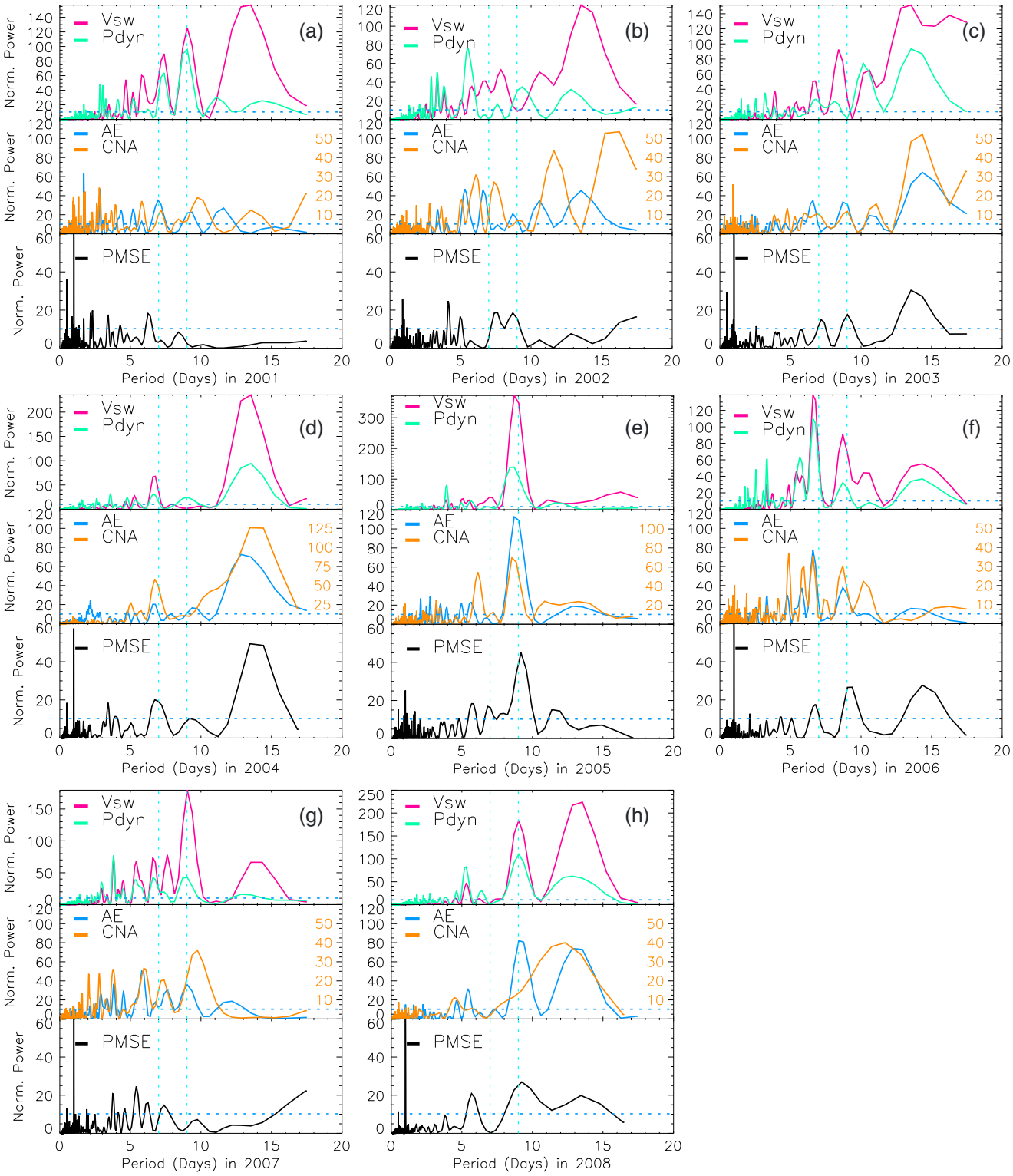

Figure 1. (a–h) Periodograms of (top) solar wind speed (Vsw, red) and solar wind dynamic pressure (Pdyn, green), (middle) auroral electrojet (*AE*) index (blue) and cosmic noise absorption (CNA, orange), and (bottom) PMSE (black) from 2001 to 2008 during the declining solar cycle. The two vertical dotted lines on each panel indicate 7 day and 9 day periods, respectively. The horizontal dotted line (blue) indicates 95% confidence level.

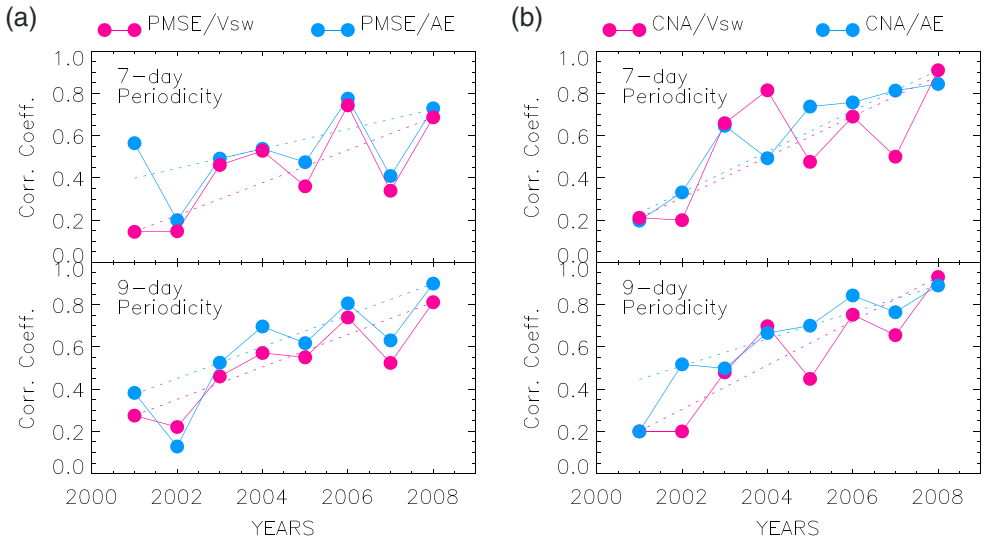

Figure 2. Correlation of (top) 7 day and (bottom) 9 day periodicities for (a) PMSE with solar wind speed (Vsw) (red) and *AE* (blue) and (b) CNA with Vsw (red) and *AE* (blue) in terms of years 2001–2008. For the correlations, 7 day (9 day) periodic time series are obtained by band-pass filtering centered at 7 day (9 day) with lower and upper bounds of 6 and 8 days (8 and 10 days). (Figure 2a) For 7 and 9 day periodicity correlation coefficients of PMSE with *AE* index, the blue dotted lines are linear fits of $y = 0.04\,x - 92$ and $y = 0.07\,x - 149$, respectively, to blue curves, and with Vsw, the red dotted lines are fitted to red curves as functions of $y = 0.07\,x - 154$ and $y = 0.07\,x - 153$, respectively. (Figure 2b) For 7 and 9 day periodicity correlation coefficients of CNA with *AE* index, the blue dotted lines are linear fits of $y = 0.09\,x - 192$ and $y = 0.06\,x - 126$, respectively, to blue curves, and with Vsw, the red dotted lines are fitted to red curves as functions of $y = 0.09\,x - 191$ and $y = 0.1\,x - 208$, respectively.

3. Results

3.1. PMSE Periodicity

In solar minimum years (2005–2008), 7, 9, and 13.5 day periodic signatures have been found in solar wind speed, *AE* index, and PMSE [e.g., *Lei et al.*, 2008b; *Thayer et al.*, 2008; *Lee et al.*, 2013]. The *AE* index is defined by the superposed *H* component plots from auroral zone magnetic observatories, specifying the geomagnetic disturbance state of both magnetosphere and ionosphere by proxy. It is obtained from total auroral electrojet currents given by $AE = AU - AL$ (westward electrojet current is subtracted from eastward electrojet current) [*Davis and Sugiura*, 1966]. Here the year-to-year variation of PMSE and *D* region ionization periodicities in days are sought for northern summer, 29 May to 08 August (day number = 150–220), during the solar declining cycle of 2001–2008. The annual results for the analysis are presented in Figure 1. Each panel of Figure 1 shows periodograms of (top) solar wind parameters of solar wind speed (Vsw) and dynamic pressure (Pdyn), (middle) *AE* index and CNA as a proxy of the level of *D* and *E* region ionization, and (bottom) PMSE volume reflectivity (η). The Lomb-Scargle periodogram analysis can be used for the estimation of power spectral density for unevenly sampled data. For the periodogram analysis, hourly averaged data are used to obtain fine periodic signatures in days even though there are some gaps in hours existing in data sets of PMSE reflectivity and CNA. One of the most outstanding periodicities in the solar declining phase appears at 9 days. For 2005, 2006, and 2008, strong 9 day periodicity occurs in Vsw, Pdyn, *AE* index, CNA, and PMSE. However, for 2007, although the periodic signature is found in solar parameters and *AE* index and CNA, it is not seen in PMSE. This likely implies that the PMSE creation is not only dependent on HSS-driven ionization but also on other factors (e.g., non-HSS geomagnetic disturbances, state of the neutral atmosphere, availability of meteoric dust, and charged ice particles). Another periodic signature appearing in solar wind parameters is a 7 day periodicity. For the years 2004 and 2006, Vsw, Pdyn, *AE* index, CNA, and PMSE occur with a 7 day periodicity. For the 13.5 day periodicity, both Vsw and PMSE accompanied by CNA have periodic signatures for 2003, 2004, 2006, and 2008. So the 13.5 day periodicity in PMSE occurs in most solar minimum years including the early solar minimum years (2003–2004). Significant 7, 9, and/or 13.5 day periodicities of PMSE responding to HSS mostly occur in the later part of the solar declining cycles of 2005–2006 and 2008 but are relatively weak for 2007. In this study periodicity correlation only for 7 and 9 days are only focused. In Figure 2, correlations for 7 and 9 day

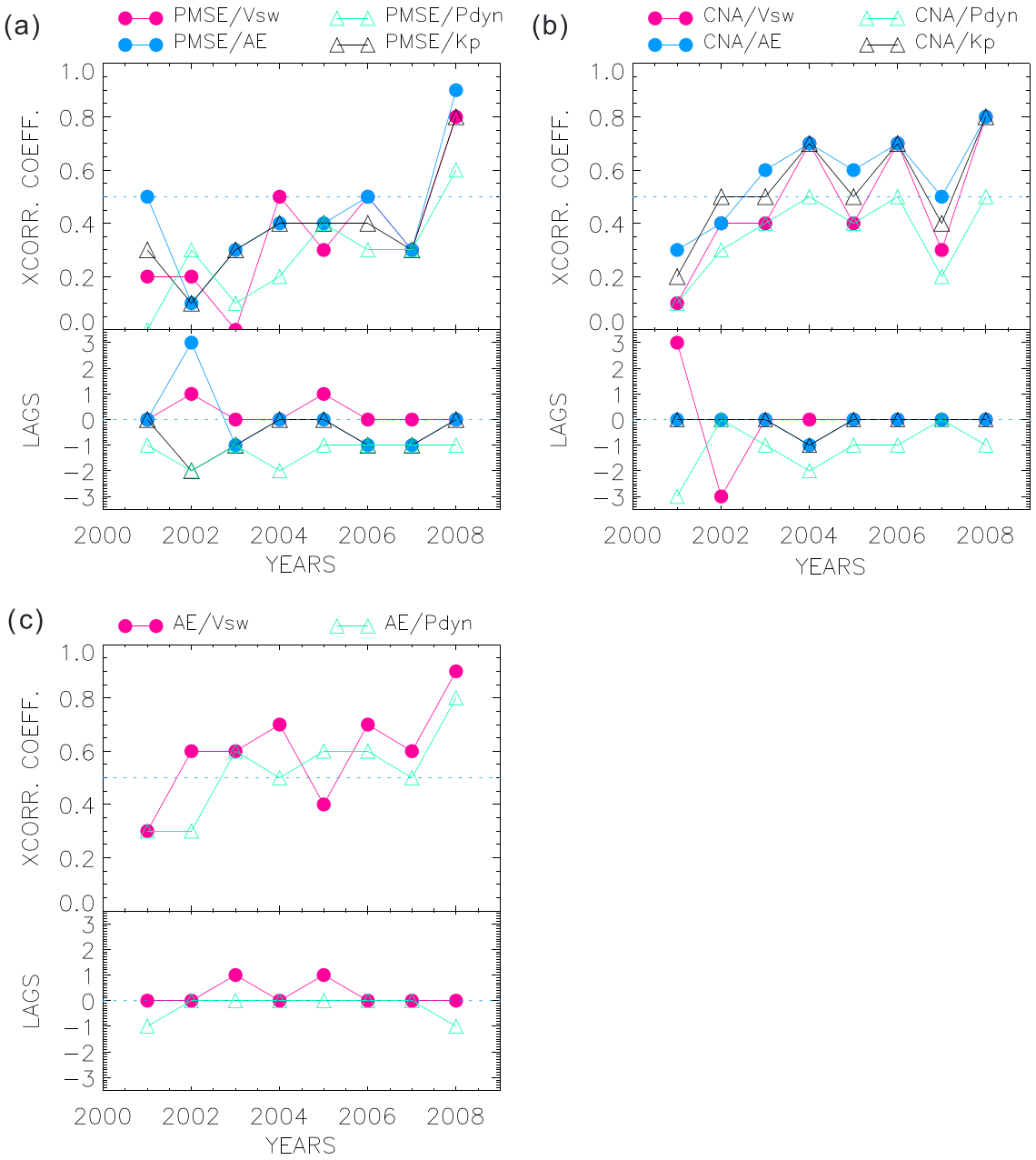

Figure 3. (a) (top) Coefficients and (bottom) lags of cross correlations of PMSE with Vsw (red), Pdyn (green), *AE* (blue), and *Kp* (black) in terms of years 2001–2008. (b) The same with Figure 3a except for CNA instead of PMSE. (c) The same operation applied for *AE* with Vsw (red) and Pdyn (green). Positive lags indicate the reciprocal parameter lagged behind PMSE and vice versa.

periodicities are plotted (Figure 2a) between PMSE and Vsw (PMSE/Vsw) and between PMSE and *AE* index (PMSE/*AE*) and (Figure 2b) between CNA and Vsw (CNA/Vsw) and between CNA and *AE* index (CNA/*AE*) in terms of years 2001–2008. For the correlations, 7 day (9 day) periodic time series are obtained by band-pass filtering centered at 7 days (9 days) with lower and upper bounds of 6 and 8 days (8 and 10 days). For PMSE 7 day periodicity with Vsw, there is much higher correlation during 2003–2008 than 2001–2002, although large year-to-year fluctuations occur. Linear fits are overplotted for the correlations in terms of years. The slopes and *y* values at year 2000 are as described in the figure captions. Here all the slopes are positive, meaning that the correlation increases as time gets closes to solar minimum (2008). The periodicity-resolved correlations of both PMSE and CNA with *AE* index are higher than those with solar wind speed as indicated (blue fitted line lying above red).

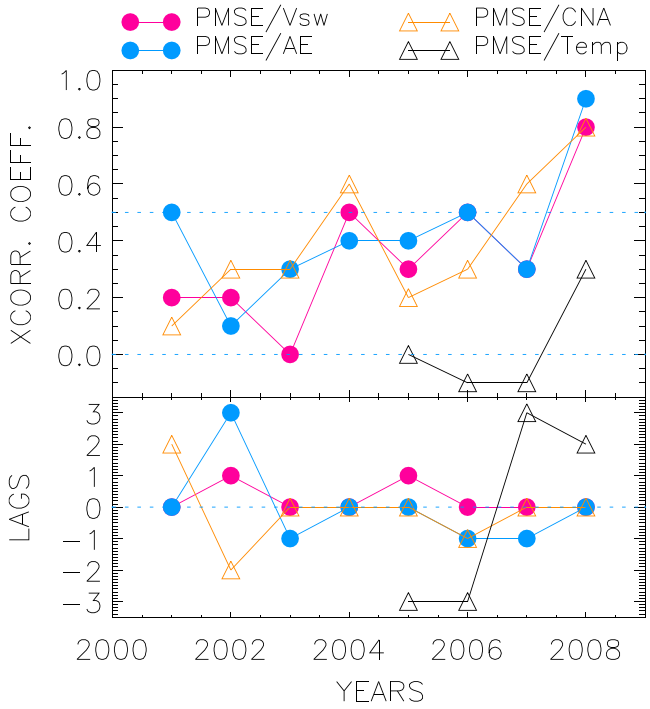

Figure 4. Correlations of PMSE with Vsw (red), CNA (orange), *AE* (blue), and temperature (black) in terms of 2001–2008.

3.2. PMSE, HSS, and *D* Region Ionization

Since the CIR is formed in front of HSS arriving at the magnetopause, solar wind density and dynamic pressure enhancements occur prior to the solar wind speed increase as observed at the L1 point by the Advanced Composition Explorer spacecraft [*Stone et al.*, 1998]. HSS-driven storms are frequently called CIR-driven (or CIR/HSS-driven) storms. The geomagnetic disturbances caused by the storms can be reflected in *AE* and *Kp* indices for high latitudes near the auroral region and middle latitudes, respectively. Thus, PMSE and *AE* peaks usually precede solar wind speed peaks as reported in *Lee et al.* [2013, 2014]. Detailed relative timing of these events is not properly represented when we have used filtered time series to separate 7 day and 9 day periodicities. Thus, correlation between PMSE and solar wind speed (or *AE* index) needs to be examined more carefully using unfiltered time series. In Figure 3a, the interannual variability of the coefficient and lag of cross correlations is shown for PMSE/Vsw (red), PMSE/Pdyn (green), PMSE/*AE* (blue), and PMSE/*Kp* (black); in Figure 3b, the same color scheme is applied for CNA; and in Figure 3c, *AE* index correlations with Vsw (red) and with Pdyn (green) are shown. Positive lags indicate the reciprocal parameter lagged behind PMSE (CNA) and vice versa. Here the dynamic pressure (Pdyn) precedes usually by 1 or 2 day PMSE, and the *AE* index peaks 1 day ahead or on the same day as PMSE. Meanwhile, the solar wind speed sometimes lags 1 day behind the PMSE by 1 day for 2002 and 2005. It is notable that the correlation of PMSE with Vsw is distinctly higher in 2004–2008 than the years of 2001–2002 solar maximum years as shown in Figure 3a. In addition, the results show that the correlation of PMSE with *AE* is better in 2001, 2003, 2005, and 2008; the same in 2006 and 2007; and lower in 2002 and 2004 than with Vsw. In solar minimum years, PMSE is as well or better correlated with *AE* than Vsw. PMSE correlation with *AE* is the same with or better than with *Kp*, which might be sometimes short of fully reflecting polar region geomagnetic effect. Besides, CNA correlates equally well with *AE*, *Kp*, Vsw, and Pdyn in years 2002, 2004, 2006, 2007, and 2008, but CNA correlates better with *AE* in 2001 and 2003. The correlation between PMSE (CNA) and Pdyn is generally lower than with the other parameters. As shown in Figure 3c, the correlation of *AE* index with Vsw is relatively larger in 2002, 2004, and 2006–2008 than with Pdyn. The effect of Pdyn on *AE* index is, as shown, comparatively higher in 2003–2008 than in 2001–2002. This likely implies that the CIR impingement drives geomagnetic disturbances. In solar maximum years, the 5 day planetary wave seems well correlated with PMSE [e.g., *Kirkwood and Rechou*, 1998; *Kirkwood et al.*, 2002], while in solar minimum years, since solar wind parameters are more effective in modulating PMSE than are planetary waves, the correlation between the temperature-modifying planetary wave feature and PMSE is less likely to be observed. Day-to-day temperature variations have been obtained for 66°N–70°N latitudes and 0°E–40°E longitudes at 87 km from MLS data. The correlation between temperature and PMSE (PMSE/Temp) is very small compared to those of PMSE/*AE* and PMSE/CNA as shown in Figure 4 (only from 2005 to 2008 as MLS temperature is not available before 2005). The link of PMSE to temperature is lower than to solar wind speed, *AE* index, and CNA (*D* region ionization) in 2005–2008.

4. Discussion

4.1. Interannual Variability of Periodicity Correlation

The harmonic periodicities (7, 9, and 13.5 days) of the 27 day solar rotation period have been well documented for the thermosphere and the ionosphere. In the thermosphere, periodic neutral mass density oscillations were found at periods of 9 days for the year 2005 and periods of 4–5, 6–7, and 9–11 days for 2006 at 400 km altitude by the CHAMP satellite [e.g., *Lei et al*., 2008b; *Thayer et al*., 2008; *Crowley et al*., 2008]. In the ionosphere, 9 and 7 day oscillations in global mean total electron content were observed from January 2005 to December 2006 using around 200 GPS receivers [e.g., *Lei et al*., 2008b; *Heelis and Sojka*, 2011]. *Meredith et al.* [2011] observed energetic particle precipitation driven by HSS above several 100 km. As reported above, long-lasting high-speed solar wind streams directed toward the Earth at 7, 9, and 13.5 day periodicities likely have predominant effects on the thermospheric and ionospheric modulations.

As for PMSE, it has been shown here that 7 and/or 9 day periodicities are common in deep solar minimum years, particularly in 2005–2006 and 2008, and a 13.5 day periodicity frequently occurs in the solar declining phase of 2003–2008. Much higher correlations between PMSE (CNA) and solar wind speed/*AE* index occur during 2003–2008, which are near to solar minimum years compared to the 2001–2002 solar maximum years except for that of 7 day periodicity in 2001, although the correlation for individual periodicities somewhat fluctuates in the solar minimum years. The periodicity-resolved correlations linearly increase in approaching the solar minimum years, and the fitted line for PMSE correlation with *AE* index is higher than that with Vsw. The results likely implicate CIR-driven geomagnetic disturbances as having most effect in producing the PMSE periodicities, similar to the linear increase of correlation between 9 day periodicities in thermospheric density and solar wind speed from 2002 to 2007 [*Lei et al*., 2008a].

4.2. PMSE Dependence on Solar Wind Parameters

Pc5 ULF wave generation increases from the solar wind dynamic pressure enhancement or CIR impingement, which is driven by high-speed solar wind streams pressing on lower speed streams, and continues with high-speed streams passing over the Earth's magnetosphere [*Elkington et al*., 1999; *Li et al*., 1997]. Electrons can be accelerated by the Pc5 ULF waves, to have high energy ($>$30 keV), even up to relativistic levels (0.5 MeV), finally precipitating into the atmosphere [*Rostoker et al*., 1998]. It is well established that dayside aurora can be caused by the solar wind dynamic pressure enhancement [*Boudouridis et al*., 2007; *Zhou and Tsurutani*, 1999; *Liou et al*., 2013; *Tsurutani et al*., 2006]. As shown in Figure 3a, it is distinctive that the correlation of PMSE with Vsw is higher in solar minimum years than solar maximum years, suggesting that precipitating high-energy particles driven by high-speed solar wind streams and the preceding CIRs likely have an effect on PMSE production. Meanwhile, as shown in Figures 3a and 3b, in the solar minimum years, PMSE and CNA correlation with *AE* index is mostly higher than with Vsw, meaning that the effect of the pressure enhancement, accompanied by the formation of CIR, on PMSE and *D* region ionization possibly precedes the solar wind speed increase. As shown in Figure 4, PMSE correlation with CNA is largest in some years (2002, 2004, and 2007), while PMSE correlation with the *AE* index is larger than with CNA in 2001, 2005–2006, and 2008. This may imply that, although PMSE can be accompanied by atmospheric ionization, they sometimes sensitively respond to precipitating electrons before the significant ionization of the atmosphere can be induced. PMSE reflectivity can be effectively improved by charged meteor smoke particles, charged ice particles, and electron density gradients [e.g., *Varney et al*., 2011; *Friedrich et al*., 2012; *Robertson et al*., 2014]. However, time constants for heterogeneous reactions in the mesosphere especially during the geomagnetic disturbance driven by HSS are not well known but challenged for the future research.

5. Summary and Conclusions

We have presented variations of periodicity-resolved correlation and total cross correlation of PMSE with solar wind speed, solar wind dynamic pressure, cosmic noise absorption (CNA), and atmospheric temperature at 84 km altitude for the declining phase of solar cycle 23 (2001–2008). The results can be summarized as follows:

1. The 7 day and 9 day periodicities in PMSE significantly occur in 2004 and 2006, and in 2005, 2006, and 2008, respectively, predominant as approaching solar minimum years. The periodicity correlation of PMSE with solar wind speed or *AE* index increases close to solar minimum years. The correlation with *AE* index, which includes geomagnetic disturbance effects of both solar wind dynamic pressure and speed, is higher than with solar wind speed.
2. The total cross correlations of PMSE and CNA with solar wind speed and *AE* index are higher in solar minimum years (2005–2008) and the declining year (2004) compared to as near to solar maximum years (2001–2003) except for 2001 with PMSE. The significant effect of HSS on *D* region ionization likely originates from the corotating interaction region impingement and high solar wind speed.
3. As far as solar minimum years (2005–2008), the correlation of PMSE with *AE* index is mostly comparable or higher than that with CNA or the solar wind speed. Therefore, HSS-induced high-energy particles possibly have strong influence on CNA, but not as much as on PMSE, especially for the years having the periodic signatures (2005–2006 and 2008).
4. Correlation of PMSE with temperature is very small and lower than HSS effect in 2005–2008 solar minimum years.

Acknowledgments

This research was supported by "Planetary system research for space exploration" project and the basic research funding from KASI, as well as sponsored by the Air Force Research Laboratory, under agreement FA2386-14-1-4004. ESRAD is a joint venture between Swedish Institute of Space Physics and Swedish Space Corporation, Esrange. We thank the GSFC/SPDF OMNIWeb for the provision of the solar wind parameters and geomagnetic activity indices used in this report. We also give thanks to GES/DISC for the provision of MLS/AURA temperature data. The contact for ESRAD data is available at website http://www.irf.se/program/paf/. The information of cosmic noise absorption data for a site of Abisko can be obtained at website www.sgo.fi.

Alan Rodger thanks the reviewers for their assistance in evaluating this paper.

References

Baker, D. N., J. B. Blake, D. J. Gorney, P. R. Higbie, R. W. Klebesadel, and J. H. King (1987), Highly relativistic magnetospheric electrons: A role in coupling to the middle atmosphere?, *Geophy. Res. Lett.*, *14*, 1027–1030, doi:10.1029/GL014i010p01027.

Barabash, V., S. Kirkwood, and P. B. Chilson (2002), Are variations in PMSE intensity affected by energetic particle precipitation?, *Ann. Geophys.*, *20*, 539–545.

Blake, J. B., W. A. Kolasinski, R. W. Fillius, and E. G. Mullen (1992), Injection of electrons and protons with energies of tens of MeV into *L*~3 on March 24, 1991, *Geophys. Res. Lett.*, *19*, 821–824, doi:10.1029/92GL00624.

Boudouridis, A., L. R. Lyons, E. Zesta, and J. M. Ruohoniemi (2007), Dayside reconnection enhancement resulting from a solar wind dynamic pressure increase, *J. Geophys. Res.*, *112*, A06201, doi:10.1029/2006JA012141.

Bremer, J., P. Hoffmann, and T. L. Hansen (2000), Geomagnetic control of polar mesosphere summer echoes, *Ann. Geophys.*, *18*, 202–208.

Chilson, P. B., S. Kirkwood, and A. Nilsson (1999), The Esrange MST radar: A brief introduction and procedure for range validation using balloons, *Radio Sci.*, *34*(2), 427–436, doi:10.1029/1998RS900023.

Cho, J. Y. N., and J. Röttger (1997), An updated review of polar mesosphere summer echoes: Observation, theory, and their relationship to noctilucent clouds and subvisible aerosols, *J. Geophys. Res.*, *102*(D2), 2001–2020, doi:10.1029/96JD02030.

Crowley, G., A. Reynolds, J. P. Thayer, J. Lei, L. J. Paxton, A. B. Christensen, Y. Zhang, R. R. Meier, and D. J. Strickland (2008), Periodic modulations in thermospheric composition by solar wind high-speed streams, *Geophys. Res. Lett.*, *35*, L21106, doi:10.1029/2008GL035745.

Davis, T. N., and M. Sugiura (1966), Auroral electrojet activity index *AE* and its universal time variations, *J. Geophys. Res.*, *71*, 785, doi:10.1029/JZ071i003p00785.

Echer, E., W. D. Gonzalez, B. T. Tsurutani, and A. L. C. Gonzalez (2008), Interplanetary conditions causing intense geomagnetic storms ($Dst < 100$ nT) during solar cycle 23 (1996–2006), *J. Geophys. Res.*, *113*, A05221, doi:10.1029/2007JA012744.

Ecklund, W. L., and B. B. Balsley (1981), Long-term observations of the arctic mesosphere with the MST radar at Poker Flat, Alaska, *J. Geophys. Res.*, *86*, 7775–7780, doi:10.1029/JA086iA09p07775.

Elkington, S. R., M. K. Hudson, and A. A. Chan (1999), Acceleration of relativistic electrons via drift-resonant interaction with toroidal-mode Pc-5 ULF oscillations, *Geophys. Res. Lett.*, *26*(21), 3273–3276, doi:10.1029/1999GL003659.

Friedrich, M., M. Rapp, T. Blix, U.-P. Hoppe, K. Torkar, S. Robertson, S. Dickson, and K. Lynch (2012), Electron loss and meteoric dust in the mesosphere, *Ann. Geophys.*, *30*, 1495–1501, doi:10.5194/angeo–30–1495–355.

Heelis, R. A., and J. J. Sojka (2011), Response of the topside ionosphere to high-speed solar wind streams, *J. Geophys. Res.*, *116*, A11314, doi:10.1029/2011JA016739.

Hunsucker, R. D. (1991), *Radio Techniques for Probing the Terrestrial Ionosphere*, Springer, Berlin.

Kavanagh, A. J., F. Honary, E. F. Donovan, T. Ulich, and M. H. Denton (2012), Key features of >30 keV electron precipitation during high speed solar wind streams: A superposed epoch analysis, *J. Geophys. Res.*, *117*, A00L09, doi:10.1029/2011JA017320.

Kim, H.-J., K. C. Kim, D.-Y. Lee, and G. Rostoker (2006), Origin of geosynchronous relativistic electron events, *J. Geophys. Res.*, *111*, A03208, doi:10.1029/2005JA011469.

Kirkwood, S., and A. Réchou (1998), Planetary-wave modulation of PMSE, *Geophys. Res. Lett.*, *25*, 4509–4512, doi:10.1029/1998GL900198.

Kirkwood, S., V. Barabash, B. U. E. Brandstrom, A. Mostrom, K. Stebel, N. Mitchell, and W. Hocking (2002), Noctilucent clouds, PMSE and 5 day planetary waves: A case study, *Geophys. Res. Lett.*, *29*, 1411, doi:10.1029/2001GL014022.

Kirkwood, S., E. Belova, P. Dalin, M. Mihalikova, D. Mikhaylova, D. Murtagh, H. Nilsson, K. Satheesan, J. Urban, and I. Wolf (2013), Response of polar mesosphere summer echoes to geomagnetic disturbances in the southern and northern hemispheres: The importance of nitric oxide, *Ann. Geophys.*, *31*, 333–347, doi:10.5194/angeo-31-333-2013.

Krieger, A. S., A. F. Timothy, and E. C. Roelof (1973), A coronal hole and its identification as the source of a high velocity solar wind stream, *Sol. Phys.*, *23*, 123.

Lee, Y.-S., S. Kirkwood, G. G. Shepherd, Y.-S. Kwak, and K.-C. Kim (2013), Long-periodic strong radar echoes in summer polar *D* region correlated with the oscillations of high-speed solar wind streams, *Geophys. Res. Lett.*, *40*, 1–5, doi:10.1002/grl.50821.

Lee, Y.-S., S. Kirkwood, Y.-S. Kwak, K.-C. Kim, and G. G. Shepherd (2014), Polar summer mesospheric extreme horizontal drift speeds during interplanetary corotating interaction regions (CIRs) and high-speed solar wind streams: Coupling between the solar wind and the mesosphere, *J. Geophys. Res. Space Physics*, *119*, 3883–3894, doi:10.1002/2014JA019790.

Lei, J., J. P. Thayer, J. M. Forbes, E. K. Sutton, R. S. Nerem, M. Temmer, and A. M. Veronig (2008a), Global thermospheric density variations caused by high-speed solar wind streams during the declining phase of solar cycle 23, *J. Geophys. Res.*, *113*, A11303, doi:10.1029/2008JA013433.

Lei, J., J. P. Thayer, J. M. Forbes, Q. Wu, C. She, W. Wan, and W. Wang (2008b), Ionosphere response to solar wind high-speed streams, *Geophys. Res. Lett.*, *35*, L19105, doi:10.1029/2008GL035208.

Li, X., D. N. Baker, M. Ternerin, D. Larson, R. P. Lin, G. D. Reeves, M. Looper, S. G. Kanekal, and R. A. Mewaldt (1997), Are energetic electrons in the solar wind the source of the outer radiation belt?, *Geophys. Res. Lett.*, *24*(8), 923–926, doi:10.1029/97GL00543.

Liou, K., D. Han, and H. Yang (2013), Ionospheric response to solar wind pressure pulses under northward IMF conditions, *Terr. Atmos. Ocean. Sci.*, *24*(2), 183–195.

Longden, N., M. H. Denton, and F. Honary (2008), Particle precipitation during ICME-driven and CIR-driven geomagnetic storms, *J. Geophys. Res.*, *113*, A06205, doi:10.1029/2007JA012752.

McComas, D. J., H. A. Elliott, J. T. Gosling, D. B. Reisenfeld, R. M. Skoug, B. E. Goldstein, M. Neugebauer, and A. Balogh (2002), Ulysses second fast latitude scan: Complexity near solar maximum and the reformation of polar coronal holes, *Geophys. Res. Lett.*, *29*(9), 1290, doi:10.1029/2001GL014164.

Meredith, N. P., R. B. Horne, M. M. Lam, M. H. Denton, J. E. Borovsky, and J. C. Green (2011), Energetic electron precipitation during high-speed solar wind stream driven storms, *J. Geophys. Res.*, *116*, A05223, doi:10.1029/2010JA016293.

Morris, R. J., M. B. Terkildsen, D. A. Holdsworth, and M. R. Hyde (2005), Is there a causal relationship between cosmic noise absorption and PMSE?, *Geophys. Res. Lett.*, *32*, L24809, doi:10.1029/2005GL024568.

Newnham, D. A., P. J. Espy, M. A. Clilverd, C. J. Rodger, A. Seppälä, D. J. Maxfield, P. Hartogh, K. Holmén, and R. B. Horne (2011), Direct observations of nitric oxide produced by energetic electron precipitation into the Antarctic middle atmosphere, *Geophys. Res. Lett.*, *38*, L20104, doi:10.1029/2011GL048666.

Pizzo, V. J. (1985), Interplanetary shocks on the large scale: A retrospective on the last decade's theoretical efforts, in *Collisionless Shocks in the Heliosphere: Reviews of Current Research*, *Geophys. Monogr. Ser*, vol. 35, edited by B. T. Tsurutani and R. G. Stone, p. 51, AGU, Washington, D. C.

Robertson, S., S. Dicksom, M. Horanyi, Z. Sternovsky, M. Friedrich, D. Janches, L. Megner, and B. Williams (2014), Detection of meteoric smoke particles in the mesosphere by a rocket-borne mass spectrometer, *J. Atmos. Sol. Terr. Phys.*, *118*, 161–179.

Rostoker, G., S. Skone, and D. N. Baker (1998), On the origin of relativistic electrons in the magnetosphere associated with some geomagnetic storms, *Geophys. Res. Lett.*, *25*, 3701–3704, doi:10.1029/98GL02801.

Smirnova, M., E. Belova, and S. Kirkwood (2011), Polar mesosphere summer echo strength in relation to solar variability and geomagnetic activity during 1997–2009, *Ann. Geophys.*, *29*, 563–572, doi:10.5194/angeo-29-563-201.

Smith, E. J., and J. H. Wolfe (1976), Observations of interaction regions and corotating shocks between 1 and 5 AU: Pioneer-10 and Pioneer-11, *Geophys. Res. Lett.*, *3*, 137–140, doi:10.1029/GL003i003p00137.

Stone, E. C., A. M. Frandsen, R. A. Mewaldt, E. R. Christian, D. Margolies, J. F. Ormes, and F. Snow (1998), The advanced composition explorer, *Space Sci. Rev.*, *86*(1–4), 1–22.

Thayer, J. P., J. Lei, J. M. Forbes, E. K. Sutton, and R. S. Nerem (2008), Thermospheric density oscillations due to periodic solar wind high-speed streams, *J. Geophys. Res.*, *113*, A06307, doi:10.1029/2008JA013190.

Tsurutani, B. T., and W. D. Gonzalez (1997), The interplanetary causes of magnetic storms: A review, in *Magnetic Storms*, edited by B. T. Tsurutani et al., AGU, Washington, D. C.

Tsurutani, B. T., W. D. Gonzalez, A. L. C. Gonzalez, F. Tang, J. K. Arballo, and M. Okada (1995), Interplanetary origin of geomagnetic activity in the declining phase of the solar cycle, *J. Geophys. Res.*, *100*, 21,717–21,734, doi:10.1029/95JA01476.

Tsurutani, B. T., A. J. Mannucci, B. A. Lijima, A. Komjathy, A. Saito, T. Tsuda, O. P. Verkhoglyadova, W. D. Gonzalez, and F. L. Guarnieri (2006), Dayside ionospheric (GPS) response to corotating solar wind streams, in *Recurrent Magnetic Storms: Corotating Solar Wind Streams*, vol. 167, 245 pp., AGU Monogr., Washington, D. C.

Varney, R. H., M. Kelley, M. C. Nicholls, C. J. Heinselman, and R. L. Collins (2011), The electron density dependence of polar mesosphere summer echoes, *J. Atmos. Sol. Terr. Phys.*, *73*, 2153–2165.

Zeller, O., and J. Bremer (2009), The influence of geomagnetic activity on mesospheric summer echoes in middle and polar latitudes, *Ann. Geophys.*, *27*, 831–837. [Available at www.ann-geophys.net/27/831/2009/.]

Zhou, X.-Y., and B. T. Tsurutani (1999), Rapid intensification and propagation of the dayside aurora: Large scale interplanetary pressure pulses (fast shocks), *Geophys. Res. Lett.*, *26*, 1097–1100, doi:10.1029/1999GL900173.